GGA1-mediated endocytic traffic of LR11/SorLA alters APP intracellular distribution and amyloid-β production

Jeremy H. Herskowitz[a], Katrin Offe[a], Aniruddha Deshpande[a], Richard A. Kahn[b], Allan I. Levey[a], and James J. Lah[a]
[a]Center for Neurodegenerative Disease, Department of Neurology, and [b]Department of Biochemistry, Emory University School of Medicine, Atlanta, GA 30322

ABSTRACT **Proteolytic processing of the amyloid-β precursor protein (APP) and generation of amyloid-β peptide (Aβ) are key events in Alzheimer's disease (AD) pathogenesis. Cell biological and genetic evidence has implicated the low-density lipoprotein and sorting receptor LR11/SorLA in AD through mechanisms related to APP and Aβ production. Defining the cellular pathway(s) by which LR11 modulates Aβ production is critical to understanding how changes in LR11 expression affect the development of Aβ pathology in AD progression. We report that the LR11 ectodomain is required for LR11-mediated reduction of Aβ and that mutagenesis of the LR11 Golgi-localizing, γ-adaptin ear homology domain, ADP-ribosylation factor (GGA)-binding motif affects the endosomal distribution of LR11, as well as LR11's effects on APP traffic and Aβ production. Targeted small interfering RNA (siRNA) knockdown studies of GGA1, GGA2, and GGA3 indicate a surprising degree of specificity toward GGA1, suggesting that GGA1 is a candidate regulator of LR11 traffic. Additional siRNA knockdown experiments reveal that GGA1 is necessary for both LR11 and β-site APP-cleaving enzyme-1 (BACE1) modulation of APP processing to Aβ. Mutagenesis of BACE1 serine 498 to alanine enhances BACE1 targeting to LR11-positive compartments and nullifies LR11-mediated reduction of Aβ. On basis of these results, we propose that GGA1 facilitates LR11 endocytic traffic and that LR11 modulates Aβ levels by promoting APP traffic to the endocytic recycling compartment.**

Monitoring Editor
Adam Linstedt
Carnegie Mellon University

Received: Jan 9, 2012
Revised: May 9, 2012
Accepted: May 16, 2012

INTRODUCTION

The amyloid-β precursor protein (APP) and its derivative, amyloid-β peptide (Aβ), play central roles in Alzheimer's disease (AD). Aβ accumulates in senile plaques, a pathological hallmark of AD (Masters *et al.*, 1985), and single-gene mutations in APP cause familial AD by altering APP processing and Aβ production (Goate *et al.*, 1991; Citron *et al.*, 1992). To generate Aβ, APP is cleaved by β-secretase/β-site of APP-cleaving enzyme-1 (BACE1), resulting in secreted APPβ (APPsβ) and a carboxyl-terminal fragment (CTFβ), and subsequent action of γ-secretase on CTFβ releases Aβ (Hussain *et al.*, 1999; Sinha and Lieberburg, 1999; Vassar *et al.*, 1999; Wolfe *et al.*, 1999; Yan *et al.*, 1999; Lin *et al.*, 2000; Xia *et al.*, 2000). Cell biological studies indicate that APP processing is determined by its intracellular traffic and exposure to secretase enzymes and that Aβ is produced in the endosomal compartment, as well as in the early secretory pathway (Sisodia, 1992; Koo and Squazzo, 1994; Hartmann *et al.*, 1997; Xu *et al.*, 1997).

Although specific gene mutations can cause familial AD, the causes of sporadic AD remain unclear. The best-established genetic risk factor is the ε4 allele of apolipoprotein E (*APOE*; Corder *et al.*, 1993; Strittmatter *et al.*, 1993). Moreover, members of the low-density lipoprotein receptor (LDLR) family, which bind ApoE, have been implicated in AD (Okuizumi *et al.*, 1995; Kang *et al.*, 1997; Ma *et al.*,

This article was published online ahead of print in MBoC in Press (http://www.molbiolcell.org/cgi/doi/10.1091/mbc.E12-01-0014) on May 23, 2012.

Address correspondence to: James J. Lah (jlah@emory.edu).

Abbreviations used: Aβ, amyloid-β peptide; AD, Alzheimer's disease; APP, amyloid-β precursor protein; BACE1, β-site APP-cleaving enzyme-1; ELISA, enzyme-linked immunosorbent assay; GGA, Golgi-localizing, γ-adaptin ear homology domain, ADP-ribosylation factor; HEK, human embryonic kidney; LDLR, low-density lipoprotein receptor; LR11, low-density lipoprotein receptor with 11 class A ligand-binding repeats.

© 2012 Herskowitz *et al.* This article is distributed by The American Society for Cell Biology under license from the author(s). Two months after publication it is available to the public under an Attribution–Noncommercial–Share Alike 3.0 Unported Creative Commons License (http://creativecommons.org/licenses/by-nc-sa/3.0).
"ASCB®," "The American Society for Cell Biology®," and "Molecular Biology of the Cell®" are registered trademarks of The American Society of Cell Biology.

2002). Low-density lipoprotein receptor with 11 class A ligand-binding repeats (LR11)/SorLA is a multidomain LDLR family member that contains structural elements that also place it in the vacuolar protein sorting 10 protein (VPS10p) homology domain family of intracellular sorting receptors (Jacobsen *et al.*, 1996). We first identified LR11 as a transcript that was down-regulated in microarray studies examining gene expression in patients with AD (Scherzer *et al.*, 2004). Subsequently, we demonstrated preferential neuronal loss of LR11 protein in brain regions vulnerable to AD pathology in sporadic but not familial AD patients, suggesting that LR11 loss plays a specific role in the pathogenesis of sporadic AD (Scherzer *et al.*, 2004; Dodson *et al.*, 2006). More recent studies indicate early loss of neuronal LR11 in individuals with mild cognitive impairment, a condition that often represents prodromal AD (Sager *et al.*, 2007). Single-nucleotide polymorphisms in noncoding regions of *SORL1*, the gene encoding LR11, have been linked to AD risk, implying that they influence disease by altering expression levels rather than by producing variant forms of LR11 (Rogaeva *et al.*, 2007).

Several reports revealed insights into the mechanism by which LR11 may influence AD pathogenesis. Overexpression of LR11 results in a highly consistent, dose-dependent reduction in APP processing to Aβ (Andersen *et al.*, 2005; Offe *et al.*, 2006; Schmidt *et al.*, 2007). Conversely, reduced LR11 expression, as occurs in sporadic AD brain, increases Aβ levels in cultured cells and accelerates amyloid pathology in a transgenic mouse model of AD (Rogaeva *et al.*, 2007; Dodson *et al.*, 2008; Rohe *et al.*, 2008). LR11 interacts with APP, and colocalization between these proteins has been observed in endosomal and Golgi compartments in multiple cell types, including primary neurons (Andersen *et al.*, 2005; Offe *et al.*, 2006; Spoelgen *et al.*, 2006). LR11 is a large transmembrane protein, and its domain structure indicates that it may act as an endocytic cell surface receptor and as an intracellular sorting receptor (Jacobsen *et al.*, 1996, 2001, 2002). The LR11 ectodomain harbors a cluster of 11 type A ligand-binding repeats and a Vps10p homology domain (Jacobsen *et al.*, 1996; Yamazaki *et al.*, 1996), and the LR11 cytoplasmic tail possesses a Golgi-localizing, γ-adaptin ear homology domain, ADP-ribosylation factor (GGA)–binding domain, found on proteins that shuttle between the *trans*-Golgi network (TGN) and endosomes, as well as an acidic amino acid cluster that regulates LR11 endocytosis (Jacobsen *et al.*, 2002; Nielsen *et al.*, 2007). Biochemical studies in vitro suggest that lumenal domain interactions mediate LR11–APP binding through the LR11 cluster of type A ligand-binding repeats (Andersen *et al.*, 2006), and another report indicates that LR11 may interact with APP via cytosolic motifs (Spoelgen *et al.*, 2006). On the basis of the lumenal domain interactions of LR11 and APP, we hypothesize that LR11 acts as an endosomal chaperone to increase APP traffic in a nonamyloidogenic pathway. However, which of the many LR11 domains are important for LR11 effects on Aβ levels remains to be determined.

Previous reports showed that changes in LR11 expression can affect APP traffic, proteolytic processing, and Aβ production (Andersen *et al.*, 2005; Offe *et al.*, 2006; Spoelgen *et al.*, 2006; Rogaeva *et al.*, 2007; Schmidt *et al.*, 2007). However, several of these studies evaluated LR11 effects in nonhuman cell lines under conditions of APP "Swedish mutant" (APP_{swe}) or APP_{695} overexpression. The APP Swedish mutation accelerates BACE1 cleavage of APP and may circumvent the need for an optimal pH environment (i.e., lumen of endosomes) for BACE1 processing of APP (Citron *et al.*, 1992; Hsiao *et al.*, 1996). Under these conditions, the intracellular sites of APP processing could change and thereby nullify or accentuate the effect(s) of other proteins, like LR11, that are involved in modulating APP processing to Aβ. In this report, we examine the role different LR11 domains play in regulating endogenous APP traffic and Aβ production in a human cell line. Modified LR11 constructs demonstrate the essential role of the LR11 ectodomain in redistributing APP to endosomes and reducing Aβ secretion. Single amino acid substitutions in the LR11 GGA-binding domain establish the requirement for this motif with respect to LR11 traffic and its effects on Aβ production and APP distribution. Targeted small interfering RNA (siRNA) knockdown experiments reveal that GGA1 regulates LR11 endocytic traffic and that GGA1 is critical for BACE1 and LR11's effects on endogenous Aβ production. On the basis of these studies, we propose that LR11 endocytic traffic, facilitated by GGA1, is critical for LR11 modulation of APP traffic and the generation of Aβ.

RESULTS

The LR11 ectodomain is required for LR11-mediated Aβ reduction

To assess the affect of the ectodomain or cytoplasmic tail of LR11 on Aβ production, we constructed two chimeras in which the ectodomain or cytoplasmic domain of LR11 was replaced with that of human LDLR, thus generating LDLR-LR11 and LR11-LDLR, respectively (Figure 1A). LDLR was chosen because it is in the same lipoprotein receptor family as LR11 and was reported to have no effect on APP processing or Aβ levels (Fryer *et al.*, 2005). In addition, we generated a construct consisting of the LR11 transmembrane and cytoplasmic domains but lacking the entire ectodomain (LR11ΔED). All constructs were epitope tagged with V5 at the N-termini.

To investigate effects on APP processing and Aβ production, we transiently expressed LR11 constructs in human embryonic kidney (HEK) 293 cells. This cell line was chosen due to the ability to detect endogenous APP protein by immunoblot and secreted Aβ by enzyme-linked immunosorbent assay (ELISA), and our standard transfection efficiency is ~60% under these conditions. Cell extracts and conditioned media were assayed for endogenous full-length APP and α-secretase cleaved APPs, respectively, by immunoblotting, and secreted Aβ1-40 was detected by sandwich ELISA. None of the LR11 constructs significantly altered the levels of full-length, cell-associated APP or APPs in the conditioned media as compared with vector (pcDNA3.1; Figure 1B). Conversely, Aβ1-40 levels were reduced by 42% of controls in cells transfected with LR11; however, Aβ1-40 levels in conditioned media were similar in vector-, LDLR-LR11–, and LR11ΔED-expressing cells (Figure 1C). Cells transfected with LR11-LDLR exhibited a 19% reduction in Aβ levels, which was significantly different from both vector- and LR11-transfected cells. These results indicate that the LR11 ectodomain is required for LR11 modulation of Aβ production, whereas the cytoplasmic domain is necessary to achieve the full effect. Control experiments demonstrate that LR11, but not LDLR, has an effect on Aβ1-40 levels, and the V5 tag did not alter this effect (Supplemental Figure S1).

Mutagenesis of the LR11 GGA-binding domain alters LR11's effects on Aβ production and APP traffic

The observation that the LR11 ectodomain is essential for LR11-mediated Aβ reduction supports our hypothesis that LR11 directs APP traffic into a nonamyloidogenic pathway through lumenal domain interactions. Short sorting motifs in the LR11 cytoplasmic tail (or other single pass receptor) dictate binding to specific regulators of intracellular traffic. These include an acidic cluster that is required for AP-2 complex–dependent endocytosis and a GGA-binding domain found on proteins, such as sortilin and mannose 6-phosphate receptors, that shuttle between the TGN and endosomes (Jacobsen *et al.*, 1996, 2001, 2002; Puertollano *et al.*, 2001; Zhu *et al.*, 2001; Doray *et al.*, 2002a, 2002b; Nielsen *et al.*, 2007).

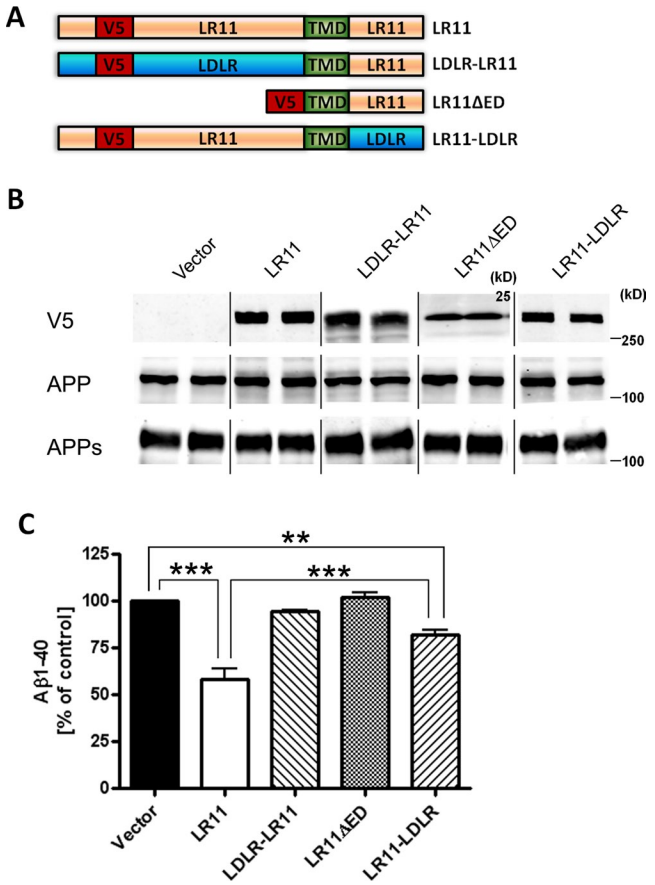

FIGURE 1: The LR11 ectodomain is required and the LR11 cytoplasmic tail is necessary for LR11-mediated reduction of Aβ. (A) Schematic representation of the N-terminal V5 epitope–tagged LR11 constructs. The V5 tag is indicated in red, and the transmembrane domain is green. The LR11 ectodomain and cytoplasmic tail are peach colored, and the LDLR ectodomain and cytoplasmic tail are blue. To analyze the effects of the LR11 ectodomain on Aβ production, we generated LDLR-LR11 and LR11ΔED, in which the LR11 ectodomain was replaced by that of LDLR or deleted, respectively. LR11-LDLR was generated to assess the requirement of the LR11 cytoplasmic domain, which was replaced with that of LDLR, on Aβ production. Not drawn to scale. (B) Effects of LR11 ectodomain and cytoplasmic domain on full-length, cell-associated APP and APPs. HEK293 cells were transfected with vector (pcDNA3.1), LR11, LDLR-LR11, LR11ΔED, or LR11-LDLR and harvested after 72 h. Media were conditioned for 48 h beginning 24 h after transfection. Equivalent volumes of conditioned media per sample and 50 μg of protein for cell lysate analyses were loaded for SDS–PAGE. Immunoblot analyses of conditioned media and cell lysate indicate similar levels of endogenous APPs and APP, respectively, among all samples. Immunoblot of cell lysate with V5 antibody indicated similar expression levels of all LR11 constructs. (C) Effects of LR11 ectodomain and cytoplasmic domain on endogenous secreted Aβ1-40. ELISA revealed that expression of LR11 reduced secreted Aβ1-40 levels by 42%, whereas expression of LR11-LDLR reduced secreted Aβ1-40 levels by only 19%, compared with vector control. Expression of LDLR-LR11 or LR11ΔED had no observable effect on secreted Aβ1-40. Values are shown as mean ± SEM (error bars). ***$p < 0.001$; **$p < 0.01$. Data shown are representative of three independent experiments.

To test whether these motifs affect LR11 effects on endogenous Aβ production, we used site-directed mutagenesis to substitute alanines for residues comprising the LR11 acidic cluster or GGA-binding domain (Figure 2A). The acidic cluster, responsible for

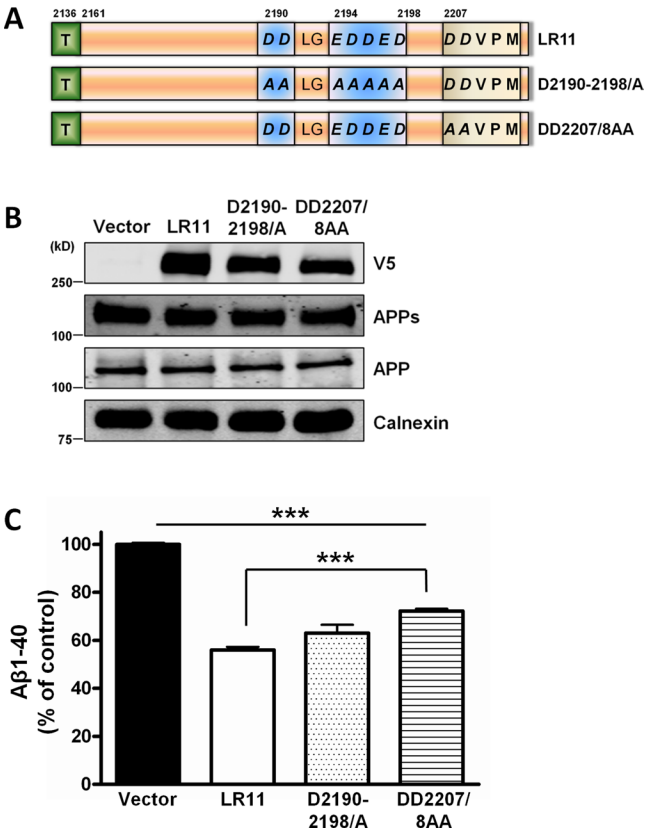

FIGURE 2: The LR11 GGA-binding domain is necessary for LR11-mediated reduction of Aβ. (A) Schematic representation of the cytoplasmic tail of N-terminal, V5 epitope–tagged LR11 constructs harboring point mutations in the LR11 acidic cluster/internalization motif or GGA-binding domain. The transmembrane domain is green. Amino acids comprising the acidic cluster/internalization motif (Nielsen *et al.*, 2007) are highlighted in blue, and five aspartic acid and two glutamic acid residues were mutated to alanines to generate D2190-2198/A. The residues involved in GGA binding are highlighted in brown, and the two aspartic acids required for GGA binding (Jacobsen *et al.*, 2002) were mutated to alanines to generate DD2207/8AA. Not drawn to scale. (B) Effects of expressing LR11 cytoplasmic tail mutants on full-length, cell-associated APP and α-secretase cleaved secreted APP. HEK293 cells were transfected with vector (pcDNA3.1), LR11, D2190-2198/A, or DD2207/8AA and harvested after 72 h. Media were conditioned for 48 h beginning 24 h after transfection. Equivalent volumes of conditioned media per sample and 50 μg of protein for cell lysate analyses were loaded for SDS–PAGE. Immunoblot analyses of conditioned media and cell lysate indicate similar levels of endogenous APPs and APP, respectively, among all samples. Immunoblot of cell lysate with V5 antibody indicated reduced levels of D2190-2198/A and DD2207/8AA compared with LR11; calnexin was used as an immunoblot loading control. (C) Effects of expressing LR11 cytoplasmic tail mutants on Aβ. ELISA revealed that expression of LR11 or D2190-2198/A reduced endogenous secreted Aβ1-40 levels by 44 and 37%, respectively, compared with vector, whereas expression of DD2207/8AA reduced secreted Aβ1-40 by only 27%. Values are shown as mean ± SEM (error bars). ***$p < 0.005$. Data shown are representative of three independent experiments.

LR11 endocytosis, comprises amino acids 2190, 2191, and 2194–2198 (DD–EDDED; Nielsen *et al.*, 2007); these five aspartic acid and two glutamic acid residues were mutated to alanines, generating D2190-2198/A. The GGA-binding domain comprises amino acids 2207–2211 (DDVPM). The two aspartic acid residues

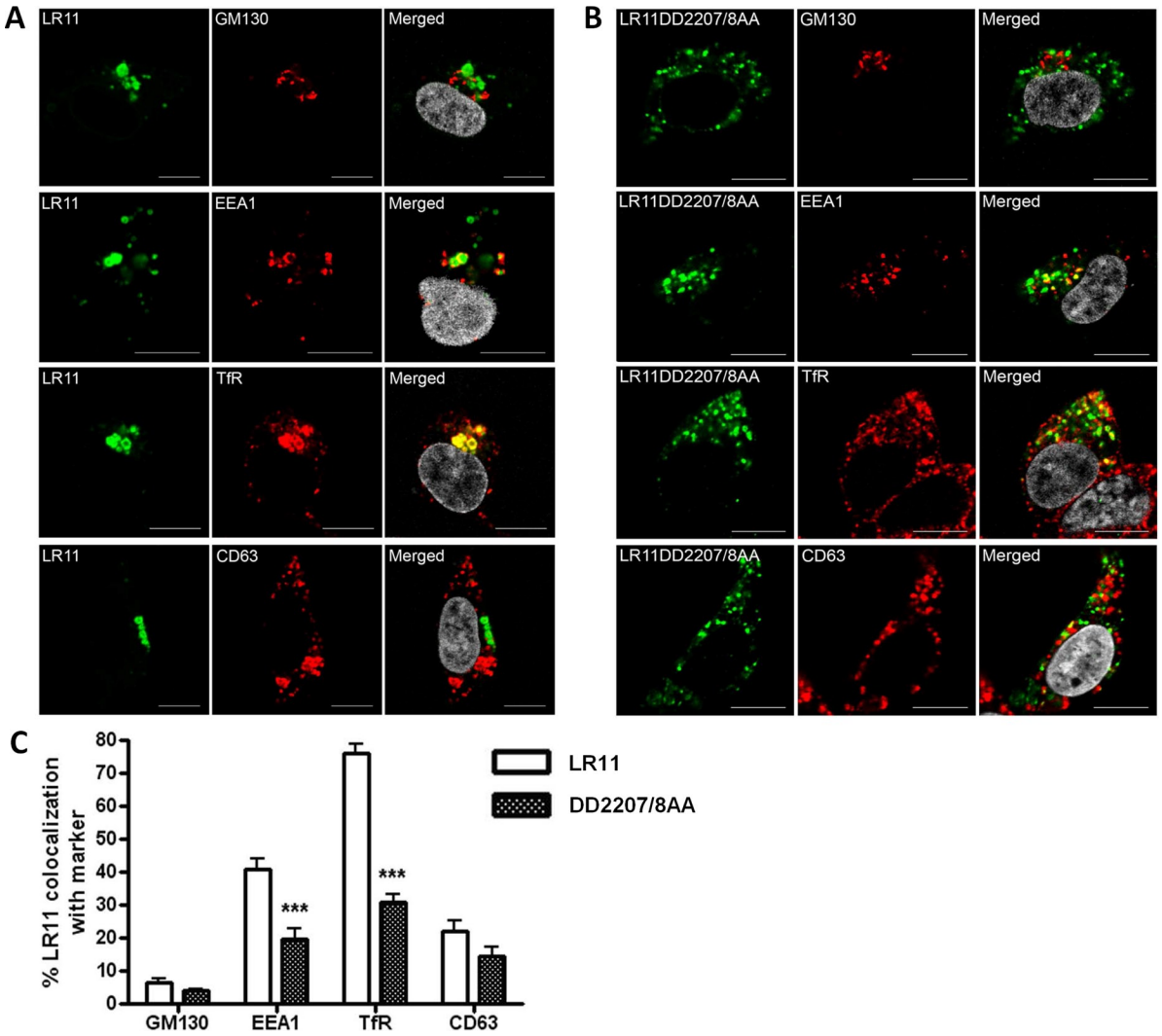

FIGURE 3: The LR11 GGA-binding domain mediates LR11 localization to the endosomal compartment. To test the effect of the LR11 GGA-binding domain on LR11 endosomal distribution, we transfected HEK293 cells with LR11 or DD2207/8AA and 24 h later plated cells on coverslips for immunofluorescence and confocal microscopy analyses. We compared colocalization of LR11 and DD2207/8AA with the following organelle markers: Golgi (GM130), sorting/early endosomes (EEA1), recycling endosomal compartment (TfR), or late endosomes/lysosomes (CD63). (A, B) Representative images of LR11 and DD2207/8AA (LR11DD2207/8AA; green) and organelle markers (red), with colocalization (yellow) shown in the merged image. (C) Quantitative analyses of LR11 and DD2207/8AA staining. DD2207/8AA overlap with EEA1 (LR11, 40.9%; DD2207/8AA, 19.7%; $p < 0.001$) and TfR (LR11, 76.1%; DD2207/8AA, 30.8%; $p < 0.001$) was significantly reduced compared with LR11. DD2207/8AA colocalization with CD63 (LR11, 22.2%; DD2207/8AA, 14.6%) and GM130 (LR11, 6.6%; DD2207/8AA,4.1%) was not significantly reduced. Values are shown as mean ± 1 SD (error bars). ***$p < 0.001$. Data shown are representative of three independent experiments. Scale bars, 10 μm.

(2207 and 2208), critical for binding GGA1 and GGA2 (Jacobsen *et al.*, 2002), were replaced with alanines, generating DD2207/8AA. LR11 constructs were transiently expressed in HEK293 cells, and cell extracts and conditioned media were assayed for endogenous full-length APP, APPs, and secreted Aβ1-40 as described for Figure 1. Expression of D2190-2198/A or DD2207/8AA had no observable effect on the levels of full-length, cell-associated APP or APPs in the conditioned media (Figure 2B). Aβ1-40 levels were reduced by 44 and 37% in cells expressing LR11 or the acidic cluster mutant, D2190-2198/A, respectively, compared with vector control (Figure 2C). Cells expressing the GGA-binding domain mutant, DD2207/8AA, displayed a blunted effect, reducing Aβ1-40 levels by 27%. The effect on Aβ1-40 levels was significantly different between LR11 and the DD2207/8AA mutant but not between LR11 and the D2190-2198/A mutant. The results in Figure 2C suggest that LR11–GGA interactions influence LR11 effects on APP processing to Aβ. However, the possibility that changes in Aβ levels are simply due to differences in LR11 and DD2207/8AA protein level cannot be ruled out.

GGA family proteins are sorting adaptors that regulate vesicle traffic between the TGN and endosomes (Boman *et al.*, 2000; Dell'Angelica *et al.*, 2000; Hirst *et al.*, 2000; Poussu *et al.*, 2000; Takatsu *et al.*, 2000). Therefore we hypothesized that mutation of the LR11 GGA-binding domain would affect LR11 endosomal distribution. To test this, we transiently transfected plasmids directing expression of LR11 or DD2207/8AA in HEK293 cells and localized LR11 and DD2207/8AA by confocal microscopy, along with markers for Golgi (GM130), early endosomes (EEA1), recycling endosomal compartment (transferrin receptor [TfR]), or late endosomes/lysosomes (CD63; Figure 3, A and B). Similar to results in previous reports

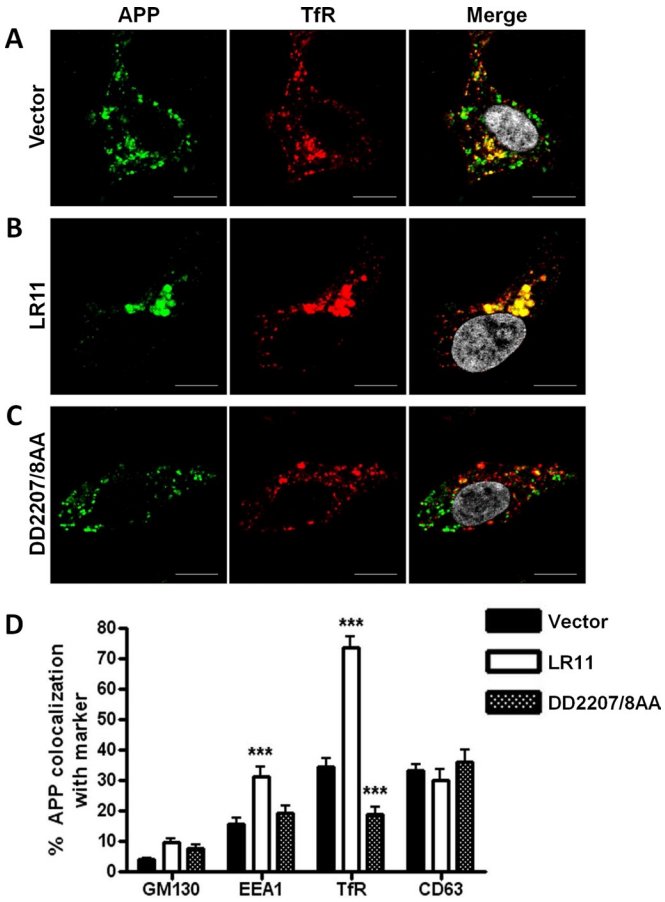

FIGURE 4: The LR11 GGA-binding domain mediates APP localization to the endosomal compartment. To test whether altered endocytic traffic of LR11 caused by mutations in its GGA-binding domain affects APP traffic, we transfected HEK293 cells with vector, LR11, or DD2207/8AA and 24 h later plated cells on coverslips for immunofluorescence and confocal microscopy analyses. We compared the effect of LR11 or DD2207/8AA expression on endogenous APP colocalization with the following organelle markers: Golgi (GM130), sorting/early endosomes (EEA1), recycling endosomal compartment (TfR), or late endosomes/lysosomes (CD63). (A–C) Representative images of APP (green) and organelle markers (red), with colocalization (yellow) shown in the merged image. (D) Quantitative analyses of endogenous APP staining in vector-, LR11-, and DD2207/8AA-transfected cells. Expressing LR11 increased APP colocalization with EEA1 (DD2207/8AA, 19.3%; LR11, 31.3%; $p < 0.05$; and vector, 15.8%) and most strongly with TfR (DD2207/8AA, 19.1%; LR11, 73.8%; $p < 0.001$; and vector, 34.5%; $p < 0.001$). Values are shown as mean ± 1 SD (error bars). ***$p < 0.001$. Data shown are representative of three independent experiments. Scale bars, 10 µm.

(Andersen *et al.*, 2005; Offe *et al.*, 2006), LR11 immunoreactivity displayed an intracellular vesicular pattern analogous to LR11 staining in primary neurons (Figure 3A). Analyses of confocal images revealed reduced colocalization of DD2207/8AA with EEA1 and TfR by 21 and 45%, respectively, compared with LR11 (Figure 3C). Conversely, DD2207/8AA overlap with CD63 and GM130 was not significantly reduced compared with LR11. These results suggest that abrogating LR11–GGA interactions reduces LR11 traffic to early and recycling endosomes. Of note, expression of LR11 induces an enlargement of TfR-positive compartments; however, pulse-chase analysis using biotinylated transferrin demonstrated that LR11 overexpression does not alter transferrin recycling kinetics (Supplemental Figure S2).

To determine whether changes in LR11 traffic caused by mutations in its GGA-binding domain affect APP traffic, we analyzed the effect of LR11 or DD2207/8AA expression on endogenous APP distribution (Figure 4, A–C). LR11 expression increased APP colocalization with EEA1 and especially TfR (Figure 4D), suggesting that LR11 promotes APP traffic to the endocytic recycling compartment. To support these findings, we also examined APP colocalization with Rab11a (Supplemental Figure S3). In contrast, expression of DD2207/8AA substantially decreased APP colocalization with TfR in comparison to LR11 and vector transfected cells. There was no observed increase in APP overlap with EEA1 under DD2207/8AA expression, and APP colocalization with GM130 and CD63 was similar among vector-, LR11-, and DD2207/8AA-transfected cells. Together, these results reveal that the LR11 GGA-binding domain plays a role in LR11-mediated effects on Aβ production and APP traffic to early endosomes and the recycling endosomal compartment.

GGA1 is a candidate regulator of LR11 traffic

Three GGAs (GGA1, GGA2, and GGA3) are each ubiquitously expressed in human cells and tissues (Boman *et al.*, 2000; Dell'Angelica *et al.*, 2000; Hirst *et al.*, 2000; Poussu *et al.*, 2000; Takatsu *et al.*, 2000). The functions of each family member and possible redundancies are not well established; some reports indicate cooperativity between GGAs, and others suggest distinct roles. Yeast two-hybrid analysis identified GGA1 and GGA2 as putative interacting partners for LR11, and GGA1 and LR11 can be coimmunoprecipitated when they are overexpressed in Chinese hamster ovary cells (Jacobsen *et al.*, 2002; Schmidt *et al.*, 2007). On the basis of our observations in experiments using LR11 GGA-binding domain mutants, we sought to identify the specific GGA family member(s) that mediates these effects.

In transfected cells, immunoblots of cell extracts showed reduced band intensity of the GGA-binding mutant (DD2207/8AA) compared with wild-type LR11 (Figure 2B). This phenotype was used to screen for the GGA family member(s) responsible. We hypothesized that absence of the requisite GGA adaptor would lead to decreased LR11 protein levels comparable to those seen with the GGA binding mutant. Immunoblot analysis was used to evaluate endogenous LR11 levels after targeted siRNA knockdown of GGA1, GGA2, or GGA3. To this end, HEK293 cells were transfected with GGA1-, GGA2-, or GGA3-targeted or control (nontargeting) siRNA smart pools, and cells were collected after 96 h to assess the efficiency of knockdown and measure changes in LR11. As seen in Figure 5, GGA1 and GGA2 were reduced to 10 and 29% of controls, respectively, whereas GGA3 was reduced to 60% of controls. Endogenous LR11 protein level was reduced to 45% of controls in GGA1-depleted cells (Figure 5, A and B); however, no effect on LR11 was observed in cells transfected with siRNA targeted to GGA2 or GGA3 (Figure 5, C and D). Reduced LR11 protein level was confirmed after RNA interference (RNAi) depletion of GGA1 using individual short hairpin RNA (shRNA) sequences (Supplemental Figure S4, A and B). A previous study of GGA family members in HeLa cells indicated that knockdown of any one GGA partially reduced the level of the other GGAs (Ghosh *et al.*, 2003). Therefore we blotted for GGA2 and GGA3 under GGA1-knockdown conditions to evaluate whether the observed effects on LR11 were due to combinatorial reductions of the GGAs. No effect on GGA2 or GGA3 was observed in cells depleted of GGA1 (Figure 5A). Although these experiments do not exclude the possibility that GGA2 and GGA3 play a role in LR11 biology, overall, the specificity of GGA1 effect on LR11 protein levels suggests that this adaptor plays a unique role in its regulation or traffic. Of note, treatment with inhibitors of

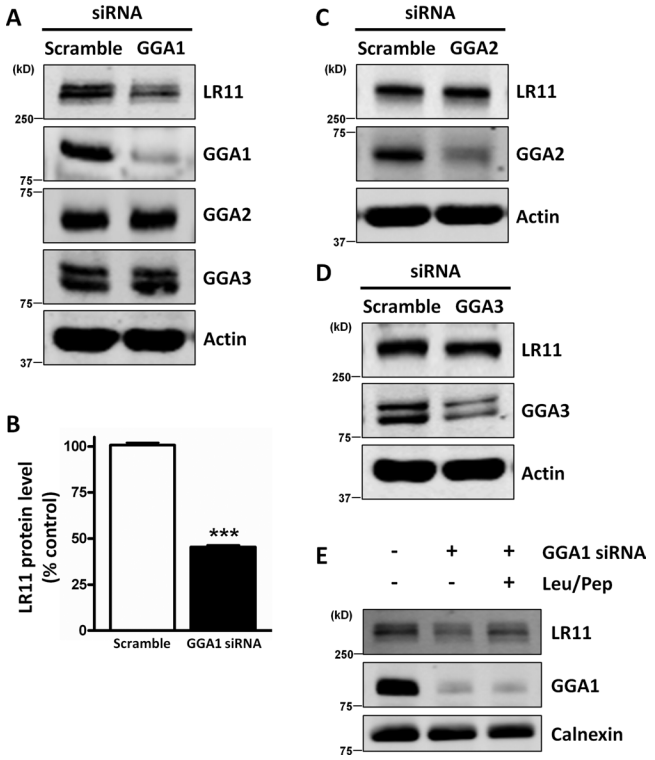

FIGURE 5: GGA1 knockdown decreases LR11 protein level. To identify the GGA family member(s) potentially involved in LR11 traffic, we used immunoblot analyses to examine endogenous LR11 protein level after targeted siRNA knockdown of GGA1, GGA2, or GGA3. (A) Targeted siRNA knockdown of GGA1. HEK293 cells were transfected with GGA1 targeted or scramble (nontargeting) siRNA smart pools and harvested after 96 h. For analyses of cell lysate, 50 μg of protein was loaded per lane in SDS–PAGE. Immunoblot analyses indicated that GGA1 was reduced to 10% of scramble controls. (B) LR11 protein level was quantified by immunoblot analyses and showed significant difference in GGA1-knockdown cells (55% decrease in LR11) compared with scramble. Values are shown as mean ± SEM (error bars). ***$p < 0.0001$. (C) Targeted siRNA knockdown of GGA2. HEK293 cells were transfected with GGA2 targeted or scramble siRNA smart pools and harvested after 96 h. GGA2 was reduced to 29% of controls; however, no effect on LR11 was observed. (D) Targeted siRNA knockdown of GGA3. HEK293 cells were transfected with GGA3 targeted or scramble siRNA smart pools and harvested after 96 h. GGA3 was reduced to 60% of controls, and no effect on LR11 was observed. β-Actin was used as an immunoblot loading control. (E) Lysosomal enzyme inhibitors prevent degradation of LR11. HEK293 cells were transfected with GGA1 targeted or scramble siRNA smart pools, and 72 h posttransfection, cells were treated with leupeptin and pepstatin (Leu/Pep) for 24 h. Depletion of GGA1 reduced LR11 to 50% of controls, and incubation with Leu/Pep increased LR11 protein level by 32%. Calnexin was used as an immunoblot loading control. Data shown are representative of three independent experiments.

lysosomal enzymes increased LR11 protein level by 32% in cells depleted of GGA1 (Figure 5E). These findings suggest that LR11 undergoes enhanced lysosomal degradation in the absence of GGA1.

On the basis of these data, we hypothesized that GGA1-mediated traffic of LR11 was necessary for LR11's effects on APP processing to Aβ. To test this hypothesis, we evaluated LR11-mediated reduction of Aβ after targeted siRNA knockdown of GGA1 in HEK293 cells. Cells were first transfected with GGA1, GGA2, or control (nontargeting) siRNA smart pools and subsequently transfected with LR11 or empty vector 24 h later. Media were conditioned for 48 h beginning 24 h after LR11 or vector transfection. The efficiency of GGA1 and GGA2 knockdown and endogenous full-length APP was analyzed by immunoblotting cell extracts, and secreted Aβ1-40 was detected by sandwich ELISA. The levels of GGA1 and GGA2 knockdown were similar to results described in Figure 5, A and C, and across all samples no observable changes in full-length APP were detected (Figure 6A). Aβ1-40 was reduced by 44% in cells transfected with control siRNA and LR11 (Figure 6B). Depleting cells of GGA1 reduced Aβ1-40 by 24%, and expressing LR11 after GGA1 knockdown produced no further effect on Aβ1-40 levels (27% reduction). These findings were confirmed after RNAi depletion of GGA1 using individual shRNA sequences (Supplemental Figure S4, C and D). Knockdown of GGA2 had no effect on levels of Aβ1-40, and expression of LR11 under these conditions lowered Aβ1-40 by 40%. These results indicate that depletion of GGA1 reduces Aβ production, and LR11's effects on Aβ levels are disrupted after knockdown of GGA1 but not GGA2.

Given the biochemical and cell biological observations with DD2207/8AA, we suspected that the loss of LR11's ability to reduce Aβ production after GGA1 depletion was the result of aberrant LR11 endocytic traffic. To test whether depletion of GGA1 affects endocytic localization of LR11, we transduced HEK293 cells with lentivirus expressing LR11 and subsequently transfected them with plasmid expressing GGA1-targeted shRNA or scramble shRNA and green fluorescent protein (GFP). Cells were plated on coverslips 72 h after transfection and fixed for immunofluorescence and confocal microscopy 24 h later. Parallel samples were transfected for 96 h with indicated plasmids and harvested for immunoblot to analyze efficiency of GGA1 knockdown (Figure 6D). Confocal images reveal that colocalization of LR11 with TfR, a marker for the endocytic recycling compartment, is disrupted under GGA1 knockdown (Figure 6C). These results, coupled with the cell biological analyses of DD2207/8AA, suggest that endocytic traffic of LR11 is impaired in the absence of GGA1 binding.

Mutagenesis of BACE1 serine 498 nullifies LR11's effects on Aβ production

Previous studies established that BACE1 interacts with the three GGAs and that GGA1 promotes BACE1 traffic from early endosomes to late endocytic compartments or the TGN (He *et al.*, 2002, 2003, 2005; von Arnim *et al.*, 2004; Wahle *et al.*, 2005). BACE1 cleavage of APP to CTFβ is optimum in acidic environments such as the lumen of endosomes and/or lysosomes (Haass *et al.*, 1992; Koo and Squazzo, 1994; Koo *et al.*, 1996; Sinha *et al.*, 1999; Vassar *et al.*, 1999; Yan *et al.*, 1999; Lin *et al.*, 2000; Sannerud *et al.*, 2011). Therefore we hypothesized that GGA1 influences BACE1's effects on Aβ production, and disruption of GGA1–BACE1 interaction may contribute to the observed reduction in Aβ after GGA1 knockdown (Figure 6B). To test this hypothesis and investigate LR11-mediated reduction of Aβ under these conditions, we evaluated BACE1's effects on endogenous Aβ production after siRNA knockdown of GGA1 in HEK293 cells. Cells were first transfected with siRNAs that targeted GGA1 or control (nontargeting) and subsequently transfected with empty vector plasmid, BACE1, or BACE1 plus LR11 24 h later. Media were conditioned for 48 h beginning 24 h after plasmid transfection. The efficiency of GGA1 knockdown and endogenous full-length APP was analyzed by immunoblotting, and secreted Aβ1-40 was detected by sandwich ELISA. The levels of GGA1 knockdown were similar to results described in Figures 5

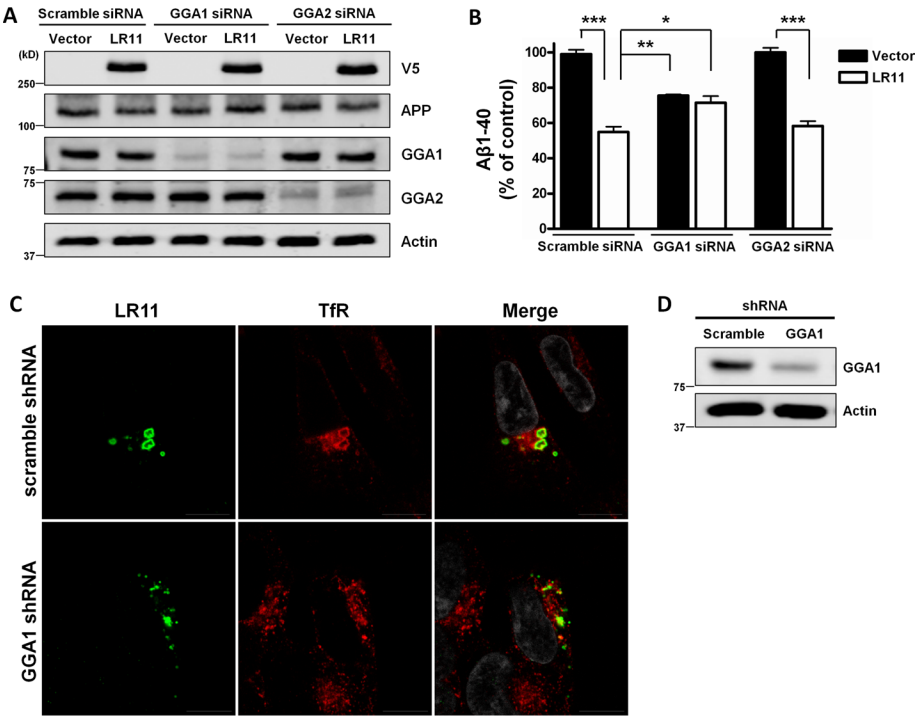

FIGURE 6: GGA1 is necessary for LR11-mediated reduction of Aβ. To determine whether GGA1 mediates LR11's effects on APP processing to Aβ, we used targeted siRNA knockdown of GGA1 in HEK293 cells and evaluated LR11-mediated reduction of Aβ . First, cells were transfected with GGA1 or GGA2 targeted or scramble (nontargeting) siRNA smart pools and subsequently transfected with vector (pcDNA3.1) or LR11 48 h. Media were conditioned for 48 h beginning 24 h after vector or LR11 transfection. (A) Immunoblot analyses of cell extract to evaluate endogenous full-length APP and efficiency of GGA1 and GGA2 knockdown. Levels of GGA1 and GGA2 knockdown were 88 and 78%, respectively, and levels of APP were similar among all samples. Immunoblot of cell lysate with V5 antibody indicated similar levels of LR11 in LR11-transfected samples. (B) Analyses of endogenous secreted Aβ1-40 by sandwich ELISA. Aβ1-40 levels were reduced by 44% from cells transfected with scramble siRNA and LR11 in comparison to vector. Targeted siRNA knockdown of GGA1 resulted in Aβ1-40 levels reduced by 24%, and expressing LR11 under GGA1 knockdown lowered Aβ1-40 levels to 27% of scramble siRNA samples. Knockdown of GGA2 had no effect on secreted Aβ1-40 levels, and expression of LR11 under these conditions lowered Aβ1-40 levels 40%. Values are shown as mean ± SEM (error bars). *p = 0.0275, **p = 0.0027, ***p = 0.0004. Data shown are representative of three independent experiments. To test whether GGA1 knockdown affects endocytic traffic of LR11, we transduced HEK293 cells with lentivirus expressing LR11 and subsequently transfected with plasmid expressing GFP and shRNA targeted against GGA1 or scramble shRNA. Cells were plated on coverslips 72 h posttransfection and fixed for immunofluorescence and confocal microscopy 24 h later. Parallel samples were harvested for immunoblot. (C) Representative images of LR11staining in scramble shRNA and GGA1 shRNA transfected cells. LR11 (green) and TfR (red), with colocalization (yellow) shown in the merged image. (D) Efficiency of GGA1 shRNA knockdown. Immunoblot analyses indicate ~57% reduction of GGA1 in GGA1 shRNA–expressing cells compared with scramble shRNA. Scale bars, 10 μm.

and 6, and across all samples no observable changes in full-length APP were detected (Figure 7A). Expression of BACE1 increased Aβ1-40 levels by 51%, whereas coexpression of BACE1 and LR11 increased Aβ1-40 levels only 29%, compared with controls (Figure 7B). These results indicate that LR11 expression can reduce endogenous Aβ levels under conditions of BACE1 overexpression. Transfection of BACE1 after GGA1 knockdown raised Aβ1-40 levels slightly above those for GGA1-depleted samples but only to levels seen in control cells, indicating that GGA1 is critical for BACE1's effects on Aβ generation. Cotransfection of LR11 and BACE1 after GGA1 knockdown produced no additional change in Aβ1-40 levels, suggesting that under these conditions, LR11-mediated reduction of Aβ is nullified.

That coexpression of LR11 with BACE1 does not affect Aβ levels under GGA1 knockdown is likely due to combinatorial effects of altered LR11 and BACE1 endocytic traffic.

Published reports established that after endocytosis, BACE1 is retrieved from early endosomes and targeted to late endosomal compartments and/or the TGN; however, reduction of GGA1 by siRNA or mutagenesis of BACE1 serine 498 (alanine substitution) leads to retention of BACE1 in early endosomes and enhances BACE1 recycling to the cell surface (Walter *et al.*, 2001; He *et al.*, 2005; Wahle *et al.*, 2005). Other studies demonstrated that phosphorylation of BACE1 serine 498 is necessary for efficient binding to GGA1 (He *et al.*, 2003; Shiba *et al.*, 2004; von Arnim *et al.*, 2004; Wahle *et al.*, 2005). Therefore, if LR11 reduces Aβ levels by mediating traffic of APP to the endocytic recycling compartment and away from early and/or late endosomes that are optimal for BACE1 cleavage of APP, then expression of BACE1S498A should disrupt this mechanism. To investigate this hypothesis, we assessed LR11-mediated reduction of secreted Aβ in the presence of BACE1S498A. Cells were transfected with the indicated plasmids, and cell extracts and conditioned media were assayed for endogenous full-length APP and secreted Aβ1-40 as described earlier. Immunoblot analyses revealed that across all samples no observable changes in full-length APP were detected (Figure 7C). Expression of BACE1 increased Aβ1-40 levels by 101%, whereas coexpression of LR11 with BACE1 blunted this effect (Figure 7D). Expressing BACE1S498A resulted in a 93% increase in Aβ1-40 levels, which was similar to results with wild-type BACE1 and consistent with previous findings (Pastorino *et al.*, 2002). Cotransfection of LR11 with BACE1S498A had no affect on Aβ1-40 levels (91% increase), indicating that LR11 action was precluded by the presence of BACE1S498A.

Previous reports demonstrated that BACE1S498A accumulates in early endosomes and exhibits enhanced endocytic recycling (Walter *et al.*, 2001; Wahle *et al.*, 2005). In this study, we show that LR11 promotes traffic of APP to the endocytic recycling compartment, and this is critical for LR11's effects on Aβ production. To investigate whether the absence of LR11-mediated reduction of Aβ in BACE1S498A-expressing cells may be due to enhanced targeting of BACE1S498A to LR11-positive compartments, we detected colocalization between BACE1 or BACE1S498A and LR11 by immunofluorescence and confocal microscopy (Figure 7E). Analyses of confocal images revealed that BACE1S498A overlap with LR11 was increased 45% compared with BACE1. Coupled with the biochemical analyses of Aβ1-40 levels described above, these results suggest that enhanced targeting of BACE1S498A to

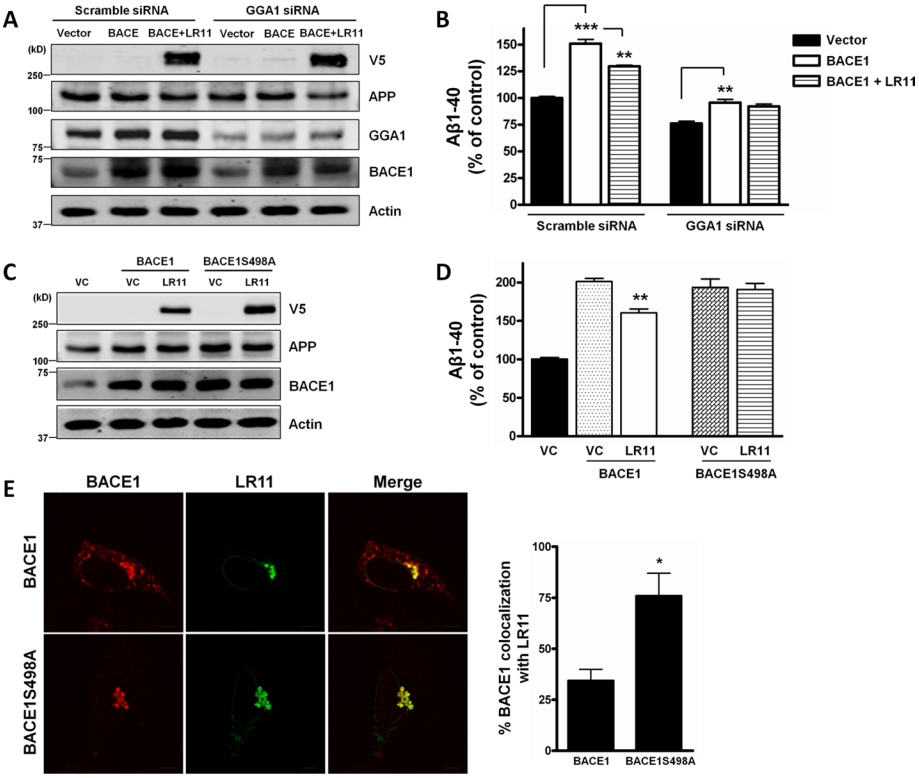

FIGURE 7: Expression of BACE1S498A nullifies LR11-mediated reduction of Aβ. To determine whether GGA1 mediates BACE1's effect on APP processing to Aβ, we used targeted siRNA knockdown of GGA1 in HEK293 cells and measured secreted Aβ1-40 levels . First, cells were transfected with GGA1 or scramble (nontargeting) siRNA smart pools and subsequently transfected with vector (pcDNA3.1), vector plus BACE1, or BACE1 plus LR11 24 h later. Media were conditioned for 48 h beginning 24 h after transfection. (A) Immunoblot analyses of cell extract to evaluate endogenous full-length APP and efficiency of GGA1 knockdown. Levels of GGA1 knockdown were comparable to reduction observed in Figure 6A, and levels of APP were similar among all samples. Immunoblot of cell lysate with V5 or BACE1 antibody indicated similar levels of LR11 and BACE1 in transfected samples. β-Actin was used as an immunoblot loading control. (B) Analyses of endogenous secreted Aβ1-40 by sandwich ELISA. Aβ1-40 levels were increased by 51% from cells transfected with scramble siRNA and BACE1, but only 29% from BACE1 plus LR11, in comparison to scramble siRNA plus vector. Targeted siRNA knockdown of GGA1 resulted in Aβ1-40 levels reduced by 23% compared with scramble siRNA plus vector. Expressing BACE1 under GGA1 knockdown increased Aβ1-40 levels to 25% over GGA1 siRNA plus vector. Coexpressing LR11 with BACE1 under GGA1 knockdown had no effect on Aβ1-40 levels compared with GGA1 siRNA plus BACE1. Values are shown as mean ± SEM (error bars). $^{**}p < 0.002$, $^{***}p < 0.0001$. Data shown are representative of three independent experiments. To determine whether LR11's effects on Aβ levels are altered in the presence of the BACE1 mutant BACE1S498A, we transfected HEK293 cells with vector, BACE1 plus vector, BACE1 plus LR11, BACE1S498A plus vector, or BACE1S498A plus LR11. Media were conditioned for 48 h beginning 24 h after transfection. (C) Immunoblot analyses of cell extract to evaluate endogenous full-length APP. Levels of APP were similar among all samples. Immunoblot of cell lysate with V5 or BACE1 antibody indicated similar levels of LR11, BACE1, or BACE1S498A in transfected samples. β-Actin was used as an immunoblot loading control. (D) Analyses of endogenous secreted Aβ1-40 by ELISA. Aβ1-40 levels were increased by 101 and 93% from cells transfected with vector and BACE1 or BACE1S498A, respectively, compared with vector alone; however, coexpression of LR11 and BACE1 increased Aβ1-40 levels only 60%. Aβ1-40 levels were similar between cells transfected with LR11 and BACE1S498A or vector and BACE1S498A. Values are shown as mean ± SEM (error bars). $^{**}p = 0.0012$. Data shown are representative of three independent experiments. To determine whether BACE1S498A localizes to LR11-positive compartments, we transfected cells with BACE1 or BACE1S498A and LR11 and plated them on coverslips for immunocytochemical analyses. (E) Representative images of BACE1 or BACE1S498A (red) and LR11 (green), with colocalization (yellow) shown in the merged image. Quantitative analyses of BACE1 or BACE1S498A and LR11 staining. BACE1S498A overlap with LR11 was significantly increased compared with BACE1 (BACE1, 34.4%; BACE1S498A, 75.9%). Values are shown as mean ± 1 SD (error bars). $^{*}p = 0.0284$. Data shown are representative of three independent experiments. Scale bars, 10 μm.

LR11-containing compartments nullifies LR11-mediated reduction of Aβ. On the basis of these studies, we propose that LR11 promotes traffic of APP in a nonamyloidogenic pathway by shunting APP away from endosomes that are optimal for BACE1 enzymatic activity.

DISCUSSION

Previous studies reported insights into the pathways by which LR11, a multifunctional low-density lipoprotein and sorting receptor, may influence AD susceptibility. Although LR11 has multiple functional domains and potential mechanisms linked to AD pathogenesis, we hypothesize that LR11 is an endosomal chaperone that increases APP traffic in a nonamyloidogenic pathway (Scherzer *et al.*, 2004; Andersen *et al.*, 2005; Offe *et al.*, 2006; Rogaeva *et al.*, 2007; Dodson *et al.*, 2008; Rohe *et al.*, 2008). To elucidate these mechanisms, it is important to better understand the functional motifs of LR11 and the proteins that regulate LR11 modulation of APP processing. Our results indicate that the LR11 ectodomain is required for LR11-mediated reduction of Aβ, and the GGA-binding domain regulates LR11 distribution in endosomal compartments and its effects on APP processing. Targeted siRNA knockdown studies of GGA isoforms reveal effects on LR11 protein levels exclusively in cells depleted of GGA1, and additional knockdown experiments show that GGA1 contributes to modulation of Aβ levels by both LR11 and BACE1. Furthermore, disrupting BACE1–GGA1 interaction or altering BACE1 endocytic targeting precludes LR11-mediated reduction of Aβ. On the basis of these observations, we conclude that endocytic traffic of LR11, facilitated by GGA1, plays a critical role in LR11 regulation of APP traffic and processing.

An important question is how LR11 affects APP distribution and traffic. To address this question, we compared colocalization of endogenous APP with organelle markers under conditions of LR11 overexpression. Expression of LR11 dramatically increased APP overlap with the endosomal markers EEA1, TfR, and Rab11a (Figure 4, A and B, and Supplemental Figure S2). TfRs and LDLR family members are well-studied cargo proteins that are regulated by clathrin-dependent endocytosis, and recycling back to the plasma membrane after endocytosis seems to be the default pathway (reviewed in Maxfield and McGraw, 2004). Although often used as a marker of recycling endosomes, TfR staining is not exclusive to a single type of endosomes and overlaps with

sorting and recycling compartments, as well as with clathrin-coated vesicles and even the TGN (Maxfield and McGraw, 2004). Of note, expression of LR11 induces an enlargement of TfR-positive compartments that is noticeably absent in cells expressing DD2207/8AA or in cells that are expressing LR11 and depleted of GGA1 (Figures 3, A and B, and 6C). Therefore it is likely that recruitment of GGAs or other adaptor proteins to LR11-containing endosomes contributes to the observed morphological changes. Previous reports concluded that LR11's effects on Aβ production occur in the perinuclear region in Golgi compartments (Spoelgen *et al.*, 2006; Schmidt *et al.*, 2007). However, our results, coupled with the analyses of Aβ secretion, suggest that it is LR11-directed traffic of APP to the endocytic recycling compartment that is critical for LR11 regulation of Aβ levels.

Previous studies examined a role for GGA1 in amyloidogenic processing of APP. APP and GGA1 were colocalized in cells overexpressing both proteins (von Arnim *et al.*, 2006; Wahle *et al.*, 2006), but glutathione *S*-transferase pull-down assays suggested that APP and GGA1 may not interact directly (Wahle *et al.*, 2006). Furthermore, Wahle *et al.* (2006) showed that siRNA knockdown of GGA1 in H4 cells overexpressing APP results in marginally increased Aβ secretion. In contrast, our studies revealed reduced Aβ secretion under endogenous conditions after siRNA depletion of GGA1 (Figure 6B). Additional siRNA knockdown experiments indicate that BACE1's effects on Aβ depend on GGA1 (Figure 7B). GGA1 mediates traffic of BACE1 between endosomes and Golgi (He *et al.*, 2002, 2003, 2005; von Arnim *et al.*, 2004; Wahle *et al.*, 2005), and therefore we hypothesize that the observed reduction of Aβ in cells depleted of GGA1 reflect impaired traffic to acidic compartments that favor BACE1 cleavage of APP to CTFβ. In addition to GGA1, BACE1's GGA-binding domain mediates interaction with and putative sorting by GGA2 and GGA3 (He *et al.*, 2002, 2003). Of note, GGA3 is believed to mediate lysosomal degradation of BACE1, and reduction of GGA3 by siRNA enhances BACE1's effects on Aβ production (Tesco *et al.*, 2007; Kang *et al.*, 2010).

Our findings with DD2207/8AA, coupled with the results of GGA1-knockdown studies, provide strong evidence that GGA1 is necessary for LR11 endocytic traffic and LR11 modulation of APP processing to Aβ. These data highlight the possibility that GGA1 mediates traffic of BACE1 and LR11 and that each pathway culminates in distinct consequences related to APP processing to Aβ. We hypothesize that GGA1 facilitates LR11 traffic to recycling endosomes; however, it is possible that GGA2 also plays a role in this mechanism. Moreover, whether GGA-mediated sorting of LR11 is direct Golgi-to-endosome traffic or shuttling between endosomal compartments remains to be determined. Reduced LR11 protein levels observed after GGA1 knockdown or mutagenesis of the GGA-binding domain may indicate that in the absence of GGA1–LR11 interaction, LR11 is targeted to degradative pathways. Jacobsen *et al.* (2002) showed in a yeast-two hybrid analysis that LR11 aspartic acids 2207 and 2208 were absolutely required for GGA1 binding. More recent studies suggest that GGA1 interaction with cargos, such as sortilin and LR11, are enhanced by phosphorylation of the serine residue that is immediately N-terminal to the cargo's GGA-binding domain (Cramer *et al.*, 2010). Our previous work demonstrated that ROCK2 phosphorylates LR11 serine 2206, which is located immediately N-terminal to the LR11 GGA-binding motif (Herskowitz *et al.*, 2011). Moreover, we showed that mutagenesis of this residue abrogated LR11-mediated reduction of Aβ. Whether or not phosphorylation of serine 2206 contributes to GGA1 interaction with LR11 in mammalian cells remains to be demonstrated.

Defining the cellular mechanism(s) by which LR11 modulates Aβ production is critical to understanding how changes in LR11 expression affect the development of amyloid pathology in sporadic AD. This report demonstrates that the LR11 ectodomain is required for LR11-mediated Aβ reduction and that the LR11 GGA-binding domain is necessary for LR11's effects on APP traffic. These data support our hypothesis that through interactions between the lumenal domain of LR11 and APP, LR11 acts as an endosomal chaperone to promote APP traffic in a nonamyloidogenic pathway. Furthermore, our studies revealed that LR11-mediated reduction of Aβ is inhibited in the presence of BACE1S498A (Figure 7D), likely due to enhanced targeting of BACE1S498A to LR11-positive compartments (Figure 7E). We propose that after endocytosis, sorting of BACE1, LR11, and APP occurs in early endosomes, and LR11 reduces Aβ production by escorting APP to the endocytic recycling compartment (Figure 8). Through this activity, LR11 shunts APP away from early and late endosomes that are optimal for BACE1 enzymatic activity. However, if LR11 promotes APP traffic to recycling compartments, why do not Aβ levels increase in the presence of BACE1S498A? It is possible that in addition to LR11's effects on APP distribution described in this report, LR11–APP complex formation confers steric hindrance against BACE1 cleavage of APP to CTFβ, as previously suggested (Spoelgen *et al.*, 2006). Elucidating the cellular mechanism(s) by which LR11 modulates APP processing to Aβ will enhance models of AD pathogenesis and provide the foundation for designing rational therapeutics that target aspects of LR11 biology, such as endocytic traffic.

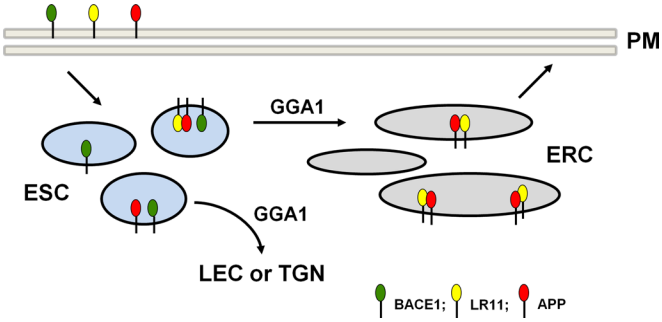

FIGURE 8: Proposed model of LR11-regulated APP traffic in a nonamyloidogenic pathway. We hypothesize that through lumenal domain interactions, LR11 acts as an endosomal chaperone to promote APP traffic in a nonamyloidogenic pathway. After internalization from the cell surface, BACE1, LR11, and APP are sorted in early endosomes (endocytic sorting compartment [ESC]), and LR11 reduces Aβ production by escorting APP to the endocytic recycling compartment (ERC). Through this activity, LR11 shunts APP away from early and late endosomes that are optimal for BACE1 enzymatic activity. GGA1 facilitates LR11 traffic to the ERC and mediates BACE1 traffic to late endosomes (late endosomal compartment [LEC]) and the TGN. PM, plasma membrane.

MATERIALS AND METHODS

Generation of expression vectors and LR11 and BACE1 mutants

Human LR11 cDNA in pcDNA3.1 (Invitrogen, Carlsbad, CA) was a gift from Chica Schaller (Zentrum für Molekulare Neurobiologie, Universität Hamburg, Hamburg, Germany), and the LDLR cDNA in a pCMV-based vector was generously provided by David Russell (Department of Molecular Genetics, University of Texas Southwestern Medical Center at Dallas, Dallas, TX). Additional constructs were designed and generated based on these cDNAs, and all were epitope-tagged with V5 at the amino terminus. All cDNA was amplified using AccuPrime Pfx DNA polymerase Supermix (Invitrogen).

LR11 cDNA was amplified using a sense primer with an *Xba*I site (5′-ATA TTC TAG AAG CGC TGC CCT GCA GCC CGA-3′) and an antisense primer introducing an *Xho*I site (5′-AAT ACT CGA GTC AGG CTA TCA CCA TGG GGA-3′). The LR11ΔED cDNA was amplified with a sense primer that introduced an *Xba*I site (5′-CCG CTC TAG ATC TAC GGA TGT TGC TGC TGT-3′) and an antisense primer containing an *Xho*I site (5′-AAT ACT CGA GTC AGG CTA TCA CCA TGG GGA-3′). To amplify full-length LDLR, the following primers were used: 5′-AGT CTC TAG AGT GGG CGA CAG ATG CGA AAG-3′, introducing an *Xba*I site, and 5′-ATG CGG CCG CTC ACG CCA CGT CAT CCT CCA-3′, introducing a *Not*I site. The LR11 ectodomain was amplified with the sense primer 5′-ATA TTC TAG AAG CGC TGC CCT GCA GCC CGA-3′, containing an *Xba*I RE site, and the antisense primer 5′-GAC CGA ATT CTC TGG CAG CCT GCG TTG CAG-3′, introducing an *Eco*RI site. The LDLR transmembrane and cytoplasmic domain for the LR11-LDLR chimera was amplified using a sense primer with an *Eco*RI site (5′-GAC CGA ATT CAG CGT GAG GGC TCT GTC CAT-3′) and an antisense primer introducing a *Not*I site (5′-ATG CGG CCG CTC ACG CCA CGT CAT CCT CCA-3′). The LDLR ectodomain was amplified with the sense primer 5′-AGT CTC TAG AGT GGG CGA CAG ATG CGA AAG-3′, containing an *Xba*I site, and the antisense primer 5′-CGC CCT CGA GAC TGG GCT TCT TCT CAT TTC-3′, containing an *Xho*I site. To generate the cytoplasmic tail of the LDLR-LR11 chimera, we amplified the LR11 transmembrane and cytoplasmic domains using the sense primer 5′-CCG CCT CGA GTC TAC GGA TGT TGC TGC TGT-3′, introducing an *Xho*I site, and the antisense primer 5′-ATG CGG CCG CTC AGG CTA TCA CCA TGG GGA-3′, introducing a *Not*I site. PCR products were cut using the appropriate restriction enzymes and ligated into modified pcDNA3.1 that contained either the LDLR signal peptide followed by V5 tag or the LR11 signal peptide followed by the LR11 propeptide and V5 tag. Correct insertions were verified by restriction digest and sequencing.

The two constructs harboring point mutations in LR11 were generated by site-directed mutagenesis using the QuikChange XL Site-Directed Mutagenesis Kit (Stratagene, La Jolla, CA) according to the manufacturer's instructions. To generate D2190-2198/A, we mutated five aspartic acid (2190, 2191, 2195, 2196, 2198) and two glutamic acid (2194, 2197) resides to alanines in the LR11 acidic cluster/internalization motif. The following primer pairs were used in succession: 5′-GAT GAC CTG GGG GAA GAT GCT GCA GAT GCC CCT ATG ATA ACT GGA and 5′-TCC AGT TAT CAT AGG GGC ATC TGC AGC ATC TTC CCC CAG GTC ATC; 5′-GAT GAC CTG GGG GCA GCT GCT GCA GAT GCC CCT ATG ATA ACT GGA and 5′-TCC AGT TAT CAT AGG GGC ATC TGC AGC AGC TGC CCC CAG GTC ATC; 5′-GAT GAC CTG GGG GCA GCT GCT GCA GCT GCC CCT ATG ATA ACT GGA and 5′- TCC AGT TAT CAT AGG GGC AGC TGC AGC AGC TGC CCC CAG GTC ATC; 5′-TCC GCA ATC TTC TCC TCT GGG GCT GCC CTG GGG GCA GCT GCT GCA and 5′-TGC AGC AGC TGC CCC CAG GGC AGC CCC AGA GGA GAA GAT TGC GGA. To generate DD2207/8A, we mutated two aspartic acid (2207, 2208) residues in the LR11 GGA-binding domain to alanines by using the following sense and antisense primers, respectively: 5′-TGA TAA CTG GAT TTT CAG CTG CCG TCC CCA TGG TGA TAG C-3′ and 5′-GCT ATC ACC ATG GGG ACG GCA GCT GAA AAT CCA GTT ATC A-3′. All LR11 point mutants were verified by sequencing. To generate lentivirus expressing LR11, we PCR amplified N-terminal V5-tagged LR11 from modified pcDNA3.1 using the primers described and ligated it into pLenti vector. Lentivirus was produced by the Emory University Viral Vector Core.

Human BACE1 cDNA in pcDNA3.1 was a gift from Robert Vassar (Northwestern University Medical School, Chicago, IL). To generate BACE1S498A, we used the following primer pair to mutate serine 498 to alanine: 5′-ACT TTG CTG ATG ACA TCG CCG CGC TGA AGT GAG GAG GCC CAT and 5′-ATG GGC CTC CTC ACT TCA GCG CGG CGA TGT CAT CAG CAA AGT. Introduction of the mutation site was verified by sequencing.

To generate expression vectors for GGA1 shRNA or scramble shRNA, we annealed the following oligos and ligated them to the pFH1UGW vector via *Bam*H1 and *Eco*RI sites. For GGA1 shRNA 1: 5′-GAT CCC ACA GGA GTG GGA GGC GAT TTC AAG AGA ATC GCC TCC CAC TCC TGT GTT TTT G and 5′-AAT TCA AAA ACA CAG GAG TGG GAG GCG AT T CTC TTG AAA TCG CCT CCC ACT CCT GTG G; for GGA1 shRNA 2: 5′-GAT CCG GGC CAG CAT CAA CGG CTT TTC AAG AGA AAG CCG TTG ATG CTG GCC CTT TTT G and 5′-AAT TCA AAA AGG GCC AGC ATC AAC GGC TTT CTC TTG AAA AGC CGT TGA TGC TGG CCC G; for scramble shRNA: 5′-GAT CCC GAT GGA GCC GGA GAC TCT TTC AAG AGA AGA GTC TCC GGC TCC ATC GTT TTT G and 5′-AAT TCA AAA ACG ATG GAG CCG GAG ACT CT T CTC TTG AAA GAG TCT CCG GCT CCA TCG G. Introduction of the GGA1 or scramble shRNA sequence was verified by restriction digest and sequencing. Expression of shRNA was driven from the H1 RNA polymerase III promoter, and the U6 promoter drove GFP expression.

Cell culture, transfection, and lentivirus transduction

HEK293 cells were maintained in DMEM with 10% fetal bovine serum (Invitrogen) and 1% penicillin/streptomycin (Cellgro/Mediatech, Herndon, VA). Equivalent amounts of cells were plated and transfected with the indicated constructs using Lipofectamine 2000 (Invitrogen) according to the manufacturer's instructions. GGA1, GGA2, and GGA3 ON-TARGETplus SMARTpool (Dharmacon, Lafayette, CO) and ON-TARGET Non-targeting Pool siRNA (Dharmacon) were transfected using DharmaFECT 1 siRNA Transfection Reagent (Dharmacon) according to the manufacturer's instructions. HEK293 cells were transduced with lentivirus expressing N-terminal V5-tagged LR11 at a multiplicity of infection of 1. For lysosomal enzyme inhibition, 0.1 μg of leupeptin and 0.05 μg of pepstatin A (both from Sigma-Aldrich, St. Louis, MO) were added per milliliter of media for 24 h (Nielsen *et al.*, 2007).

Antibodies

For detecting the V5 tag on LR11 constructs, a polyclonal V5 antibody (Sigma-Aldrich) was used for immunocytochemistry, and a monoclonal antibody to V5 (MCA1360; AbD Serotec, Raleigh, NC) was used for immunoblot. For the organelle markers in immunocytochemical experiments, the following antibodies were used: EEA1 for sorting/early endosomes and GM130 antibody for Golgi (monoclonals from Transduction Laboratories/BD Biosciences, San Jose, CA), KDEL for endoplasmic reticulum (monoclonal from Assay Designs, Ann Arbor, MI), TfR for the recycling endosomal compartment (monoclonal from Zymed/Invitrogen, San Francisco, CA), and CD63 for late endosomes/lysosomes (monoclonal from BD Biosciences PharMingen, San Diego, CA). For endogenous LR11 immunoblot, monoclonal antibody (611860) from Transduction Laboratories/BD Biosciences was used. For immunoblot and immunofluorescence of GGA1, GGA2, and GGA3, the following antibodies were used: rabbit polyclonal antisera to GGA1 were generated as described previously (Boman *et al.*, 2000), GGA2 rabbit polyclonal (ab10552) from Abcam (Cambridge, MA), and GGA3 monoclonal (612310) from Transduction Laboratories/BD Biosciences. For immunofluorescence and immunoblot of full-length, cell-associated APP and immunoblot of secreted α-secretase cleaved APP (monoclonal 6E10; Signet, SIG-39320-200; Covance, Berkeley, CA) was

used. For immunoblot loading controls, the following antibodies were used: calnexin polyclonal (SPA-860; Assay Designs, Ann Arbor, MI) and β-actin monoclonal (ab6276; Abcam). For immunofluorescence and immunoblot of BACE1 and BACE1S498A, a polyclonal BACE1 antibody (AHB0281; BioSource International, Camarillo, CA) was used. For immunoblot of biotinylated transferrin, a polyclonal goat biotin antibody (600-131-098; Rockland Immunochemicals, Gilbertsville, PA) was used.

Cell harvest and immunoblotting

Cells were lysed as previously described (Offe *et al.*, 2006; Herskowitz *et al.*, 2010) in phosphate-buffered saline (PBS) plus protease inhibitor cocktail (Roche Diagnostics, Mannheim, Germany), Halt phosphatase inhibitor cocktail (Pierce, Rockford, IL), and lysis buffer containing 0.5% NP-40, 0.5% deoxycholate, 150 mM sodium chloride, and 50 mM Tris, pH 7.4. Immunoblotting was performed as previously described (Offe *et al.*, 2006). To load equivalent amounts of soluble lysate per sample for immunoblot analyses, we determined protein concentration by bicinchoninic acid method (Pierce). Images were captured using an Odyssey Image Station (Li-Cor, Lincoln, NE), and band intensities were quantified using Scion Image. Statistical analysis was performed using Student's *t* test for independent samples.

Aβ measurements

HEK293 cells were transiently transfected with siRNA and/or indicated plasmids, and media were conditioned for 48 h beginning 24 h after final transfection. Conditioned media were collected and cells were harvested for immunoblot analyses as described. Endogenous Aβ1-40 was detected using a sandwich ELISA for human β amyloid 1-40 (Millipore, Billerica, MA) following the manufacturer's instructions. Plates were read at 450 nm on a Spectra Max Plus plate reader (Molecular Devices, Sunnyvale, CA). Cell extracts and conditioned media samples were blotted for indicated proteins as described in the text. Experiments were performed in triplicate.

Immunocytochemistry and confocal microscopy

For immunocytochemistry experiments, cells were plated onto Matrigel extracellular matrix (BD, Franklin Lakes, NJ)–coated coverslips in 12-well culture dishes 24 h after transfection. Cells plated on coverslips were fixed for 30 min in 2% paraformaldehyde and rinsed several times with PBS containing 0.5% normal horse serum, 0.5% normal goat serum, and 0.05% saponin (rinse buffer). The cells were blocked and permeabilized for 30 min with PBS containing 5% normal horse serum, 5% normal goat serum, 1% bovine serum albumin, and 0.05% saponin (blocking buffer) plus 0.05% Triton X-100. Cells were rinsed several times with rinse buffer and incubated in primary antibody diluted in blocking buffer overnight at 4°C. For double and triple labeling, two primary antibodies were included in the incubation. The next day cells were rinsed and incubated for 1 h with both fluorophore-conjugated anti-rabbit and mouse secondary antibodies (Jackson ImmunoResearch, West Grove, PA) in blocking buffer. For triple labeling, the secondary antibodies used were goat Fab fragments (Jackson ImmunoResearch). This was followed by a block with unconjugated goat anti-mouse or anti-rabbit monovalent Fab fragments. Cells were then incubated with the third primary overnight at 4°C. The next day, cells were rinsed and incubated with secondary antibody for 1 h at room temperature. After rinsing, cell nuclei were stained with Hoechst 333258 (Molecular Probes, Invitrogen, Carlsbad, CA) for 5 min, mounted onto slides using Vectashield mounting medium (Vector Laboratories, Burlingame, CA), and sealed. Control conditions included omission of one or more primary antibodies to test incomplete block, nonspecific secondary antibody binding, and bleedthrough. Controls showed negligible staining. Images were captured using an LSM510 confocal microscope (Zeiss, Thornwood, NY) and processed with Photoshop (Adobe, San Jose, CA) by manually tracing a single cell per image, as well as a 20 × 20 pixel region of the nucleus. Quantification of colocalization was performed using Matlab R2006 software (The MathWorks, Natick, MA). For each channel of the RGB image, the average pixel intensity plus 1 SD of the outlined nuclear region was measured and defined as background. The average pixel intensity plus 1 SD of the pixels in the outlined cell that were exceeding background intensity was then measured, and the threshold was set at this value. For pixels with intensities greater than threshold, the percentage of pixels in one channel overlapping with those in the other channels was calculated. The data were analyzed with two-way analysis of variance and Bonferroni post hoc tests using Prism software (GraphPad Software, San Diego, CA). The data are presented as means ± 1 SD. Experiments were performed in triplicate.

Transferrin recycling assay

HEK293 cells were plated in 60-mm dishes and subsequently transfected with indicated constructs. Twenty-four hours later the cells were split into 12-well dishes. The next day, the cells were serum starved for 1 h and then incubated with bovine serum albumin–supplemented media containing 10 μg/ml of iron-saturated biotinylated transferrin (Sigma-Aldrich) for 1 h at 37°C. Unbound and surface-bound biotinylated transferrin were removed by placing the cells on ice and washing twice with cold PBS, once with low-pH wash buffer (150 mM NaCl, 10 mM acetic acid pH 3.5), and finally twice with cold PBS. To measure transferrin recycling, we returned the cells to 37°C and incubated them in medium containing 1 mg/ml unlabeled transferrin (Sigma-Aldrich). Medium was collected at 0, 5, 10, 20, and 40 min, and the cells were harvested for immunoblot analyses as described. Recycled and cell-associated biotinylated transferrin were quantified as previously described (Kachhap *et al.*, 2007). Briefly, a fraction of lysate and corresponding media was processed for immunoblot. At each time point recycled transferrin was expressed as a percentage of total transferrin.

ACKNOWLEDGMENTS

We thank members of the Lah/Levey, Betarbet, and Kahn labs for constructive discussion regarding the manuscript, and we are grateful to Craig Heilman for technical assistance on this project. This work was supported by grants from the National Institutes of Health through the Emory NINDS Neuroscience Core Facilities (P30 NS055077), Alzheimer's Disease Research Center Grant AG025688, NINDS Training and Translational Research in Neurology Grant T32 NS007480-07 (J.H.H.), and Grants NIA P01AG1449 and R01GM067226 (R.A.K.). We acknowledge the donors of Alzheimer's Disease Research, a program of the American Health Assistance Foundation, for support of this research. Parts of this research were conducted while J.H.H was an Ellison Medical Foundation/American Federation for Aging Research Postdoctoral Fellow.

REFERENCES

Andersen OM *et al.* (2005). Neuronal sorting protein-related receptor sorLA/LR11 regulates processing of the amyloid precursor protein. Proc Natl Acad Sci USA 102, 13461–13466.

Andersen OM *et al.* (2006). Molecular dissection of the interaction between amyloid precursor protein and its neuronal trafficking receptor SorLA/LR11. Biochemistry 45, 2618–2628.

Boman AL, Zhang C, Zhu X, Kahn RA (2000). A family of ADP-ribosylation factor effectors that can alter membrane transport through the *trans*-Golgi. Mol Biol Cell 11, 1241–1255.

Citron M, Oltersdorf T, Haass C, McConlogue L, Hung AY, Seubert P, Vigo-Pelfrey C, Lieberburg I, Selkoe DJ (1992). Mutation of the beta-amyloid precursor protein in familial Alzheimer's disease increases beta-protein production. Nature 360, 672–674.
Corder EH, Saunders AM, Strittmatter WJ, Schmechel DE, Gaskell PC, Small GW, Roses AD, Haines JL, Pericak-Vance MA (1993). Gene dose of apolipoprotein E type 4 allele and the risk of Alzheimer's disease in late onset families. Science 261, 921–923.
Cramer JF, Gustafsen C, Behrens MA, Oliveira CL, Pedersen JS, Madsen P, Petersen CM, Thirup SS (2010). GGA autoinhibition revisited. Traffic 11, 259–273.
Dell'Angelica EC, Puertollano R, Mullins C, Aguilar RC, Vargas JD, Hartnell LM, Bonifacino JS (2000). GGAs: a family of ADP ribosylation factor-binding proteins related to adaptors and associated with the Golgi complex. J Cell Biol 149, 81–94.
Dodson SE, Andersen OM, Karmali V, Fritz JJ, Cheng D, Peng J, Levey AI, Willnow TE, Lah JJ (2008). Loss of LR11/SORLA enhances early pathology in a mouse model of amyloidosis: evidence for a proximal role in Alzheimer's disease. J Neurosci 28, 12877–12886.
Dodson SE, Gearing M, Lippa CF, Montine TJ, Levey AI, Lah JJ (2006). LR11/SorLA expression is reduced in sporadic Alzheimer disease but not in familial Alzheimer disease. J Neuropathol Exp Neurol 65, 866–872.
Doray B, Bruns K, Ghosh P, Kornfeld S (2002a). Interaction of the cation-dependent mannose 6-phosphate receptor with GGA proteins. J Biol Chem 277, 18477–18482.
Doray B, Ghosh P, Griffith J, Geuze HJ, Kornfeld S (2002b). Cooperation of GGAs and AP-1 in packaging MPRs at the *trans*-Golgi network. Science 297, 1700–1703.
Fryer JD *et al.* (2005). The low density lipoprotein receptor regulates the level of central nervous system human and murine apolipoprotein E but does not modify amyloid plaque pathology in PDAPP mice. J Biol Chem 280, 25754–25759.
Ghosh P, Griffith J, Geuze HJ, Kornfeld S (2003). Mammalian GGAs act together to sort mannose 6-phosphate receptors. J Cell Biol 163, 755–766.
Goate A *et al.* (1991). Segregation of a missense mutation in the amyloid precursor protein gene with familial Alzheimer's disease. Nature 349, 704–706.
Haass C, Koo EH, Mellon A, Hung AY, Selkoe DJ (1992). Targeting of cell-surface beta-amyloid precursor protein to lysosomes: alternative processing into amyloid-bearing fragments. Nature 357, 500–503.
Hartmann T *et al.* (1997). Distinct sites of intracellular production for Alzheimer's disease A beta40/42 amyloid peptides. Nat Med 3, 1016–1020.
He X, Chang WP, Koelsch G, Tang J (2002). Memapsin 2 (beta-secretase) cytosolic domain binds to the VHS domains of GGA1 and GGA2: implications on the endocytosis mechanism of memapsin 2. FEBS Lett 524, 183–187.
He X, Li F, Chang WP, Tang J (2005). GGA proteins mediate the recycling pathway of memapsin 2 (BACE). J Biol Chem 280, 11696–11703.
He X, Zhu G, Koelsch G, Rodgers KK, Zhang XC, Tang J (2003). Biochemical and structural characterization of the interaction of memapsin 2 (beta-secretase) cytosolic domain with the VHS domain of GGA proteins. Biochemistry 42, 12174–12180.
Herskowitz JH, Seyfried NT, Duong DM, Xia Q, Rees HD, Gearing M, Peng J, Lah JJ, Levey AI (2010). Phosphoproteomic analysis reveals site-specific changes in GFAP and NDRG2 phosphorylation in frontotemporal lobar degeneration. J Proteome Res 9, 6368–6379.
Herskowitz JH, Seyfried NT, Gearing M, Kahn RA, Peng J, Levey AI, Lah JJ (2011). Rho kinase II phosphorylation of the lipoprotein receptor LR11/SORLA alters amyloid-beta production. J Biol Chem 286, 6117–6127.
Hirst J, Lui WW, Bright NA, Totty N, Seaman MN, Robinson MS (2000). A family of proteins with gamma-adaptin and VHS domains that facilitate trafficking between the *trans*-Golgi network and the vacuole/lysosome. J Cell Biol 149, 67–80.
Hsiao K, Chapman P, Nilsen S, Eckman C, Harigaya Y, Younkin S, Yang F, Cole G (1996). Correlative memory deficits, Abeta elevation, and amyloid plaques in transgenic mice. Science 274, 99–102.
Hussain I *et al.* (1999). Identification of a novel aspartic protease (Asp 2) as beta-secretase. Mol Cell Neurosci 14, 419–427.
Jacobsen L, Madsen P, Jacobsen C, Nielsen MS, Gliemann J, Petersen CM (2001). Activation and functional characterization of the mosaic receptor SorLA/LR11. J Biol Chem 276, 22788–22796.
Jacobsen L, Madsen P, Moestrup SK, Lund AH, Tommerup N, Nykjaer A, Sottrup-Jensen L, Gliemann J, Petersen CM (1996). Molecular characterization of a novel human hybrid-type receptor that binds the alpha2-macroglobulin receptor-associated protein. J Biol Chem 271, 31379–31383.
Jacobsen L, Madsen P, Nielsen MS, Geraerts WP, Gliemann J, Smit AB, Petersen CM (2002). The sorLA cytoplasmic domain interacts with GGA1 and -2 and defines minimum requirements for GGA binding. FEBS Lett 511, 155–158.
Kachhap SK, Faith D, Qian DZ, Shabbeer S, Galloway NL, Pili R, Denmeade SR, DeMarzo AM, Carducci MA (2007). The N-Myc down regulated Gene1 (NDRG1) Is a Rab4a effector involved in vesicular recycling of E-cadherin. PLoS One 2, e844.
Kang DE, Saitoh T, Chen X, Xia Y, Masliah E, Hansen LA, Thomas RG, Thal LJ, Katzman R (1997). Genetic association of the low-density lipoprotein receptor-related protein gene (LRP), an apolipoprotein E receptor, with late-onset alzheimer's disease. Neurology 49, 56–61.
Kang EL, Cameron AN, Piazza F, Walker KR, Tesco G (2010). Ubiquitin regulates GGA3-mediated degradation of BACE1. J Biol Chem 285, 24108–24119.
Koo EH, Squazzo SL (1994). Evidence that production and release of amyloid beta-protein involves the endocytic pathway. J Biol Chem 269, 17386–17389.
Koo EH, Squazzo SL, Selkoe DJ, Koo CH (1996). Trafficking of cell-surface amyloid beta-protein precursor. I. Secretion, endocytosis and recycling as detected by labeled monoclonal antibody. J Cell Sci 109, 991–998.
Lin X, Koelsch G, Wu S, Downs D, Dashti A, Tang J (2000). Human aspartic protease memapsin 2 cleaves the beta-secretase site of beta-amyloid precursor protein. Proc Natl Acad Sci USA 97, 1456–1460.
Ma SL, Ng HK, Baum L, Pang JC, Chiu HF, Woo J, Tang NL, Lam LC (2002). Low-density lipoprotein receptor-related protein 8 (apolipoprotein E receptor 2) gene polymorphisms in Alzheimer's disease. Neurosci Lett 332, 216–218.
Masters CL, Simms G, Weinman NA, Multhaup G, McDonald BL, Beyreuther K (1985). Amyloid plaque core protein in Alzheimer disease and Down syndrome. Proc Natl Acad Sci USA 82, 4245–4249.
Maxfield FR, McGraw TE (2004). Endocytic recycling. Nat Rev Mol Cell Biol 5, 121–132.
Nielsen MS *et al.* (2007). Sorting by the cytoplasmic domain of the amyloid precursor protein binding receptor SorLA. Mol Cell Biol 27, 6842–6851.
Offe K, Dodson SE, Shoemaker JT, Fritz JJ, Gearing M, Levey AI, Lah JJ (2006). The lipoprotein receptor LR11 regulates amyloid beta production and amyloid precursor protein traffic in endosomal compartments. J Neurosci 26, 1596–1603.
Okuizumi K *et al.* (1995). Genetic association of the very low density lipoprotein (VLDL) receptor gene with sporadic Alzheimer's disease. Nat Genet 11, 207–209.
Pastorino L, Ikin AF, Nairn AC, Pursnani A, Buxbaum JD (2002). The carboxyl-terminus of BACE contains a sorting signal that regulates BACE trafficking but not the formation of total A(beta). Mol Cell Neurosci 19, 175–185.
Poussu A, Lohi O, Lehto VP (2000). Vear, a novel Golgi-associated protein with VHS and gamma-adaptin "ear" domains. J Biol Chem 275, 7176–7183.
Puertollano R, Aguilar RC, Gorshkova I, Crouch RJ, Bonifacino JS (2001). Sorting of mannose 6-phosphate receptors mediated by the GGAs. Science 292, 1712–1716.
Rogaeva E *et al.* (2007). The neuronal sortilin-related receptor SORL1 is genetically associated with Alzheimer disease. Nat Genet 39, 168–177.
Rohe M *et al.* (2008). Sortilin-related receptor with A-type repeats (SORLA) affects the amyloid precursor protein-dependent stimulation of ERK signaling and adult neurogenesis. J Biol Chem 283, 14826–14834.
Sager KL, Wuu J, Leurgans SE, Rees HD, Gearing M, Mufson EJ, Levey AI, Lah JJ (2007). Neuronal LR11/sorLA expression is reduced in mild cognitive impairment. Ann Neurol 62, 640–647.
Sannerud R *et al.* (2011). ADP ribosylation factor 6 (ARF6) controls amyloid precursor protein (APP) processing by mediating the endosomal sorting of BACE1. Proc Natl Acad Sci USA 108, E559–E568.
Scherzer CR, Offe K, Gearing M, Rees HD, Fang G, Heilman CJ, Schaller C, Bujo H, Levey AI, Lah JJ (2004). Loss of apolipoprotein E receptor LR11 in Alzheimer disease. Arch Neurol 61, 1200–1205.
Schmidt V, Sporbert A, Rohe M, Reimer T, Rehm A, Andersen OM, Willnow TE (2007). SorLA/LR11 regulates processing of amyloid precursor protein via interaction with adaptors GGA and PACS-1. J Biol Chem 282, 32956–32964.
Shiba T, Kametaka S, Kawasaki M, Shibata M, Waguri S, Uchiyama Y, Wakatsuki S (2004). Insights into the phosphoregulation of beta-secretase sorting signal by the VHS domain of GGA1. Traffic 5, 437–448.

Sinha S *et al*. (1999). Purification and cloning of amyloid precursor protein beta-secretase from human brain. Nature 402, 537–540.
Sinha S, Lieberburg I (1999). Cellular mechanisms of beta-amyloid production and secretion. Proc Natl Acad Sci USA 96, 11049–11053.
Sisodia SS (1992). Beta-amyloid precursor protein cleavage by a membrane-bound protease. Proc Natl Acad Sci USA 89, 6075–6079.
Spoelgen R, von Arnim CA, Thomas AV, Peltan ID, Koker M, Deng A, Irizarry MC, Andersen OM, Willnow TE, Hyman BT (2006). Interaction of the cytosolic domains of sorLA/LR11 with the amyloid precursor protein (APP) and beta-secretase beta-site APP-cleaving enzyme. J Neurosci 26, 418–428.
Strittmatter WJ, Saunders AM, Schmechel D, Pericak-Vance M, Enghild J, Salvesen GS, Roses AD (1993). Apolipoprotein E: high-avidity binding to beta-amyloid and increased frequency of type 4 allele in late-onset familial Alzheimer disease. Proc Natl Acad Sci USA 90, 1977–1981.
Takatsu H, Yoshino K, Nakayama K (2000). Adaptor gamma ear homology domain conserved in gamma-adaptin and GGA proteins that interact with gamma-synergin. Biochem Biophys Res Commun 271, 719–725.
Tesco G *et al*. (2007). Depletion of GGA3 stabilizes BACE and enhances beta-secretase activity. Neuron 54, 721–737.
Vassar R *et al*. (1999). Beta-secretase cleavage of Alzheimer's amyloid precursor protein by the transmembrane aspartic protease BACE. Science 286, 735–741.
von Arnim CA *et al*. (2006). GGA1 acts as a spatial switch altering amyloid precursor protein trafficking and processing. J Neurosci 26, 9913–9922.
von Arnim CA, Tangredi MM, Peltan ID, Lee BM, Irizarry MC, Kinoshita A, Hyman BT (2004). Demonstration of BACE (beta-secretase) phosphorylation and its interaction with GGA1 in cells by fluorescence-lifetime imaging microscopy. J Cell Sci 117, 5437–5445.
Wahle T, Prager K, Raffler N, Haass C, Famulok M, Walter J (2005). GGA proteins regulate retrograde transport of BACE1 from endosomes to the *trans*-Golgi network. Mol Cell Neurosci 29, 453–461.
Wahle T, Thal DR, Sastre M, Rentmeister A, Bogdanovic N, Famulok M, Heneka MT, Walter J (2006). GGA1 is expressed in the human brain and affects the generation of amyloid beta-peptide. J Neurosci 26, 12838–12846.
Walter J, Fluhrer R, Hartung B, Willem M, Kaether C, Capell A, Lammich S, Multhaup G, Haass C (2001). Phosphorylation regulates intracellular trafficking of beta-secretase. J Biol Chem 276, 14634–14641.
Wolfe MS, Xia W, Ostaszewski BL, Diehl TS, Kimberly WT, Selkoe DJ (1999). Two transmembrane aspartates in presenilin-1 required for presenilin endoproteolysis and gamma-secretase activity. Nature 398, 513–517.
Xia W, Ray WJ, Ostaszewski BL, Rahmati T, Kimberly WT, Wolfe MS, Zhang J, Goate AM, Selkoe DJ (2000). Presenilin complexes with the C-terminal fragments of amyloid precursor protein at the sites of amyloid beta-protein generation. Proc Natl Acad Sci USA 97, 9299–9304.
Xu H, Sweeney D, Wang R, Thinakaran G, Lo AC, Sisodia SS, Greengard P, Gandy S (1997). Generation of Alzheimer beta-amyloid protein in the *trans*-Golgi network in the apparent absence of vesicle formation. Proc Natl Acad Sci USA 94, 3748–3752.
Yamazaki H, Bujo H, Kusunoki J, Seimiya K, Kanaki T, Morisaki N, Schneider WJ, Saito Y (1996). Elements of neural adhesion molecules and a yeast vacuolar protein sorting receptor are present in a novel mammalian low density lipoprotein receptor family member. J Biol Chem 271, 24761–24768.
Yan R *et al*. (1999). Membrane-anchored aspartyl protease with Alzheimer's disease beta-secretase activity. Nature 402, 533–537.
Zhu Y, Doray B, Poussu A, Lehto VP, Kornfeld S (2001). Binding of GGA2 to the lysosomal enzyme sorting motif of the mannose 6-phosphate receptor. Science 292, 1716–1718.